3. Passive Seismic Experiment

Gary V. Latham,[a†] *Maurice Ewing,*[a] *Frank Press,*[b] *George Sutton,*[c] *James Dorman,*[a] *Yosio Nakamura,*[d] *Nafi Toksoz,*[b] *Ralph Wiggins,*[b] *and Robert Kovach*[e]

The purpose of the passive seismic experiment (PSE) is to detect vibrations of the lunar surface and to use these data to determine the internal structure, physical state, and tectonic activity of the Moon. Sources of seismic energy may be internal (moonquakes) or external (meteoroid impacts and manmade impacts). A secondary objective of the experiment is the determination of the number and the mass of meteoroids that strike the lunar surface. The instrument is also capable of measuring tilts of the lunar surface and changes in gravity that occur at the instrument location. Detailed investigation of lunar structure must await the establishment of a network of seismic stations; however, a single, large, well-recorded seismic event can provide information of fundamental importance that could not be gained by any other method.

Since deployment and activation of the PSE on November 19, 1969, the instrument has operated as planned, except as noted in the paragraphs entitled "Instrument Description and Performance." The sensor was installed west-northwest from the lunar module (LM) at a distance of 130 m from the nearest LM footpad. With the successful installation and operation of the first Apollo lunar surface experiments package (ALSEP), the feasibility of using long-lived geophysical stations to study the Moon has been demonstrated.

Signals of 40 seismic events have been identified on the records for the 42-day period following LM ascent. Of these signals, 10 are thought to be produced by noise sources within the LM descent stage. The remaining 30 signals, classified as type L, are prolonged, with gradual buildup and decrease in signal amplitude. This signal character may imply transmission with very low attenuation and intense wave scattering – conditions that are mutually exclusive on Earth. Because of the similarity with the signal from the impact of the LM ascent stage, L-signals are thought to be produced by meteoroid impacts or shallow moonquakes. Most of the L-events appear to have originated within 100 km of the ALSEP. The occurrence of similar L-events during both the Apollo 11 and Apollo 12 missions greatly strengthens the present belief that, of the various types of signals observed, L-events are the most likely to be of natural origin.

The fact that no natural seismic signals with characteristics similar to those typically recorded on the Earth were observed during the combined recording period for Apollo 11 and 12 (63 days at this writing) is a major scientific result. The high sensitivity at which the lunar instruments were operated would have resulted in the detection of many such signals if the Moon were as seismically active as the Earth and had the same transmission characteristics as the Earth. Thus, the data obtained indicate that seismic energy release is either far less for the Moon than for the Earth or that the interior of the Moon is highly attenuating for seismic waves. Although the material of the outer region of the Moon (to depths of at least 20 km) appears to exhibit very low attenuation in the regions studied, the possibility of the existence of high attenuation at greater depths cannot presently be excluded. The

[a] Lamont-Doherty Geological Observatory.
[b] Massachusetts Institute of Technology.
[c] University of Hawaii.
[d] General Dynamics, Fort Worth, Tex.
[e] Stanford University.
[†] Principal investigator.

absence of significant seismic activity within the Moon, if verified by future data, would imply the absence of tectonic processes similar to those associated with major crustal movements on the Earth and would imply lower specific thermal energy in the lunar interior than is present in the interior of the Earth.

However, it is important to remember that all results obtained thus far pertain to mare regions. Quite different results may be obtained for nonmare regions in which the lunar structure may differ radically from that in the mare.

Instrument Description and Performance

A seismometer consists simply of a mass, free to move in one direction, that is suspended by means of a spring (or a combination of springs and hinges) from a framework. The suspended mass is provided with damping to suppress vibrations at the natural frequency of the system. The framework rests on the surface whose motions are to be studied and moves with the surface. The suspended mass tends to remain fixed in space because of its own inertia while the frame moves around the mass. The resulting relative motion between the mass and the frame can be recorded and used to calculate original ground motion if the instrumental constants are known. Conventional seismic instruments are prohibitively large and delicate for use on lunar missions. For example, a typical single-axis low-frequency seismometer designed for use on Earth weighs approximately 30 kg and occupies 1×10^5 cm^3.

The Apollo 12 PSE (ref. 3–1) consists of two main subsystems: the sensor unit and the electronics module. The sensor, shown schematically in figure 3–1, contains three matched long-period (LP) seismometers (with resonant periods of 15 sec) alined orthogonally to measure one vertical and two horizontal components of surface motion. The sensor also includes a single-axis short-period (SP) seismometer (with a resonant period of 1 sec) sensitive to vertical motion at higher frequencies.

The instrument is constructed principally of beryllium and weighs 11.5 kg, including the electronics module and thermal insulation. Without insulation, the sensor is 23 cm in diameter and 29 cm high. Total power drain varies between 4.3 and 7.4 W.

Instrument temperature control is provided by a 2.5-W heater, a proportional controller, and an insulating wrapping of aluminized Mylar. The insulating shroud is spread over the local surface to reduce temperature variations of the surface material. In this way, it is expected that thermally induced tilts of the local surface will be reduced to acceptable levels.

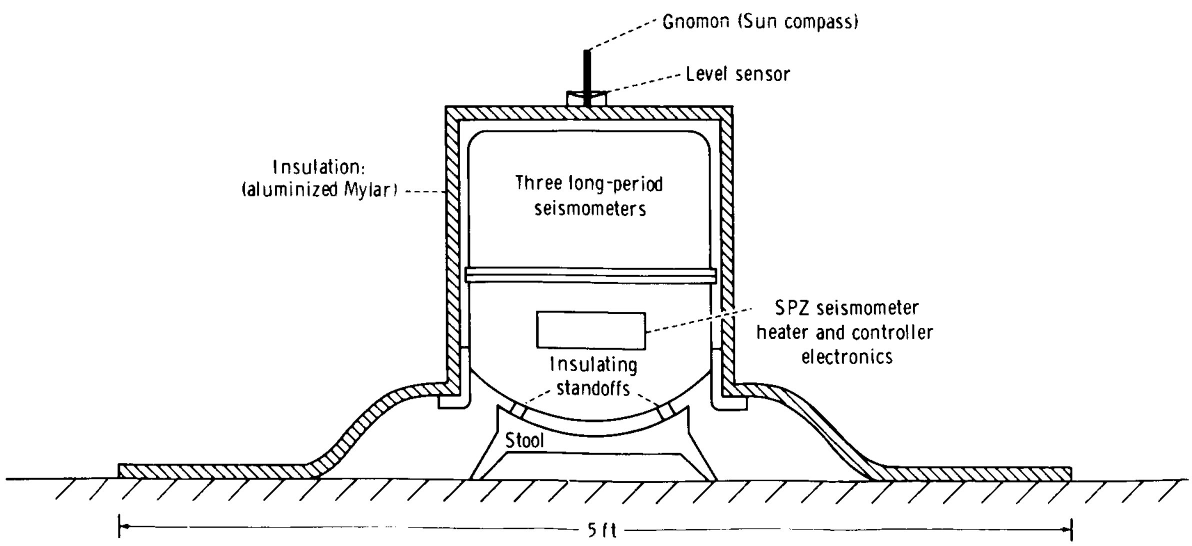

FIGURE 3-1. — Schematic diagram of the PSE sensor unit.

The LP seismometers will detect vibrations of the lunar surface in the frequency range from 0.004 to 2 Hz. The SP seismometer covers the band from 0.05 to 20 Hz. The LP seismometers can detect ground motions as small as 0.3 nm at maximum sensitivity; the SP seismometer can detect ground motions of 0.3 nm at 1 Hz.

The LP horizontal-component (LPX and LPY) seismometers are very sensitive to tilt and must be leveled to high accuracy. In the Apollo system, the seismometers are leveled by means of a two-axis motor-driven gimbal. A third motor adjusts the LP vertical-component (LPZ) seismometer in the vertical direction. Motor operation is controlled by command. These elements are shown schematically in figure 3–2. As shown in figure 3–2, the LP seismometers are mounted in crisscross fashion to reduce the required volume.

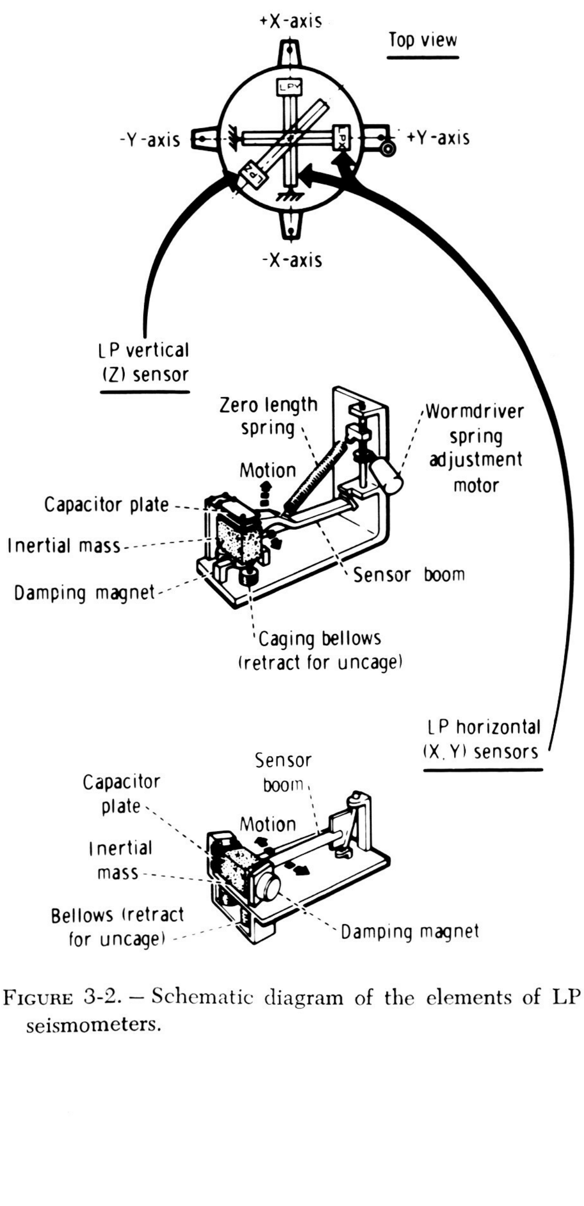

FIGURE 3-2. – Schematic diagram of the elements of LP seismometers.

Calibration of the complete system is accomplished by applying an accurate increment or step of current to the coil of each of the four seismometers by transmission of a command from Earth. The current step is equivalent to a known step of ground acceleration.

A caging system is provided to secure all critical elements of the instrument against damage during the transport and deployment phases of the Apollo mission. In the present design, a pneumatic system is used in which pressurized bellows expand to clamp fragile parts in place. Uncaging is performed on command by piercing the connecting line by means of a small explosive device.

The seismometer system is controlled from Earth by a set of 15 commands that govern functions such as speed and direction of leveling motors, instrument gain, and calibration. The seismometer is shown fully deployed on the lunar surface in figure 3–3.

The PSE instrumentation has operated successfully throughout the first 42 days of the experiment, the time period discussed in this report. The instrument difficulties that have been observed are described in the following paragraphs.

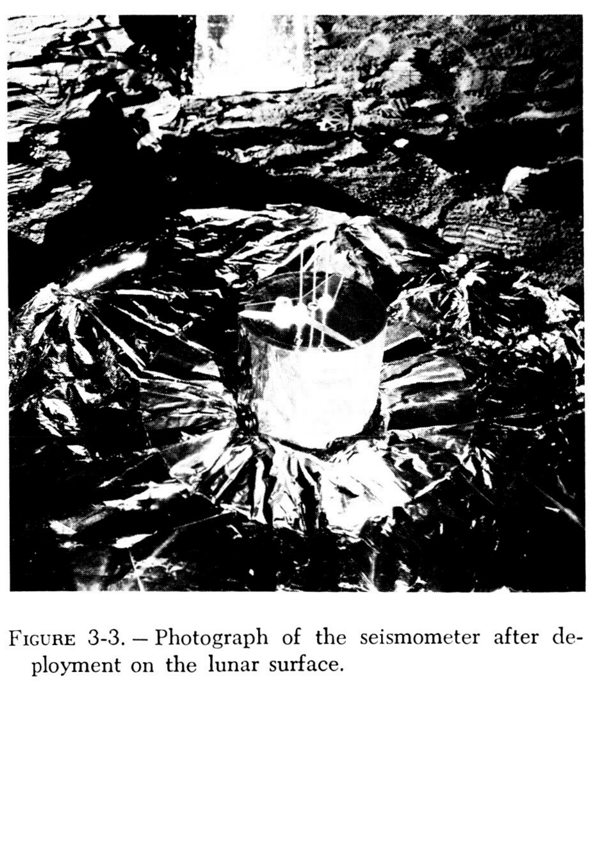

FIGURE 3-3. – Photograph of the seismometer after deployment on the lunar surface.

Short-Period Seismometer

The SPZ seismometer appears to be operating at reduced gain. The first evidence of this problem appeared when the instrument failed to respond to calibration pulses. (No calibration pulses have been detected to date on the SPZ component.) Detailed comparison between signals observed on both LPZ and SPZ seismometers has led to the tentative conclusion that the inertial mass of the SP seismometer is rubbing slightly on the frame. Response, which is apparently normal, is observed for large signals, presumably because such signals produce forces large enough to exceed the static frictional restraining forces. Restraining forces introduced by sliding friction are apparently less important. The threshold ground-motion acceleration required to produce an observable signal cannot be determined accurately; however, the smallest signals observed correspond to a surface acceleration of 8×10^{-4} cm/sec^2 (peak-to-peak surface motion amplitude of 2 nm at a frequency of 10 Hz). Lunar surface accelerations less than this approximate threshold are apparently not detected by the SPZ seismometer.

A series of square-wave pulses observed on the SPZ seismometer trace began at 11:00 G.m.t. on December 2, 1969, and lasted approximately 13 hr. A similar "storm" commenced at approximately 08:00 G.m.t. on December 28, 1969, and ended some time between 01:00 and 23:00 G.m.t. on January 1, 1970. The pulse amplitude was constant and was approximately equal to a shift in the third least-significant bit of the 10-bit binary ALSEP data word. These pulses are also observable on the records from the LP seismometers, but the pulses have reduced amplitude. The source of these pulses has not yet been identified, but malfunction of the PSE analog-to-digital (A/D) converter or of the converter reference voltage is suspected. The fact that each of these "storms" occurred just subsequent to lunar noon, that the second storm was the stronger of the two, and that the seismometer temperature rose to 142° F at the second lunar noon as compared to 134° F at the first lunar noon suggests that the high temperatures in the seismometer may have caused the trouble.

Long-Period Seismometers

The response of the LPZ seismometer to a calibration pulse was observed to be oscillatory soon after activation. This effect gradually increased to the point of instability. In the presence of feedback, this tendency toward instability can be produced if the natural period of the seismometer is lengthened (or if the feedback-filter corner period is shortened) beyond the design value. It is considered most likely, at this point in the analysis, that vibration effects lengthened the natural period of the seismometer from 15 sec to approximately 60 sec. Acceptable seismometer operation has been achieved by removing the feedback filters from all three seismometers by command. In this configuration, the seismometers have responses equal to underdamped pendulums with natural periods of 2.2 sec. The instrument response curve corresponding to this mode of operation is shown in figure 3–4.

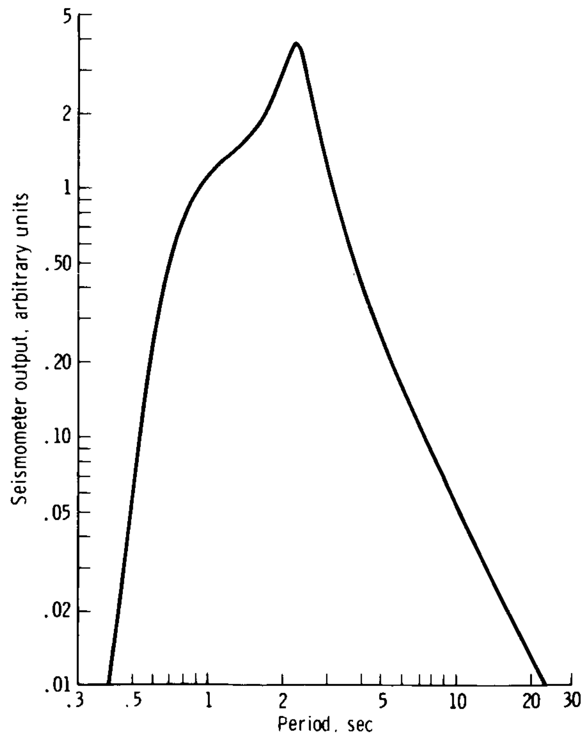

FIGURE 3-4. – Response of LP seismometers with feedback filters removed. Seismometer sensitivity for unity ordinate value is 5-mV output for 0.3-nm ground motion.

Thermal Control

The PSE active thermal control system was designed to maintain constant temperature to ±18° F about a set point of 125° F. The observed range is from +85° F (predicted by extrapolation) during the lunar night to +142° F during the lunar day. This temperature variation will not degrade the quality of seismic data but will greatly reduce the probability of obtaining useful tidal data. It appears that higher-than-anticipated heater output is required to maintain the temperature of the sensor unit within the ±18° F tolerance.

Deployment

Several points raised by the astronauts relative to the sensor emplacement are worthy of note. It appears that tamping the lunar surface material with the ribbed soles of the astronauts' boots is not an effective means of preparing the surface for experiment emplacement. The total compaction achieved by such tamping is reported to be small. Secondly, spreading the thermal shroud smoothly over the surface was difficult. The lightweight Mylar sheets of which the shroud is constructed appeared to resist a flat-lying configuration. It is not known whether this resistance is caused by electrical effects or by elastic memory within the Mylar.

Description of Recorded Seismic Signals

This experiment is a continuation of observations made during the Apollo 11 mission (refs. 3-2 and 3-3).

Preascent Period

Prior to LM ascent, many signals corresponding to various astronaut activities on the surface and within the LM were recorded, primarily on the LPZ component. The astronauts' footfalls were detectable at all points along their traverse (maximum range, approximately 360 m). Signals of particular interest were generated by test firings of the reaction control system (RCS) thrustors while the LM was on the lunar surface and by the LM ascent. Signals received from these sources are shown in figure 3-5. By measuring the elapsed time between engine ignition and signal arrival at the PSE for the RCS test firings and for the LM ascent, the compressional velocity of the lunar surface material has been determined to be approximately 108 m/sec. This value is consistent with estimates derived on the basis of mechanical properties measured by Surveyor, as presented in references 3-4 and 3-5 and by Sutton and Duennebier in "Seismic Characteristics for the Lunar Surface From Surveyor Spacecraft Data" (to be published).

Signals were also recorded from the impacts of the two portable life-support systems as they struck the lunar surface after ejection from the LM. Observed signal amplitudes from these sources are smaller by a factor of 80 than the signals observed from the same sources during Apollo 11. This reduced amplitude of the observed signals is due to the increased separation of the PSE and the LM during the Apollo 12 mission.

Postascent Period

Forty seismic signals of possible natural origin have been identified on the records for the 38-day period following LM ascent (the period for which data are available): 10 on the SPZ component and 30 on the LP components. All but one of the 10 high-frequency events detected by the SPZ component were recorded within 8 hr after LM ascent and may correspond to LM venting processes. This observation is in contrast to the thousands of signals assumed to be of LM origin that were recorded during the first 8 days of the Apollo 11 seismometer operation. This drastic reduction in the number of interfering noises from the LM is due, primarily, to the nearly eightfold increase in distance from the LM (130 m for Apollo 12 as compared to 16.8 m for Apollo 11). Part of the reduction may be attributed to the reduced sensitivity of the SPZ component to small signals.

Direct correlation has been made between signals recorded by the magnetometer (also on the lunar surface) and those recorded by the SPZ component. This correlation was particularly noticeable during passage of the ALSEP through the transition zone between the tail of the magnetic field of the Earth and interplanetary space, where rapid variations in the magnetic field were observed on the magnetometer record. It is assumed that detectable currents are induced in

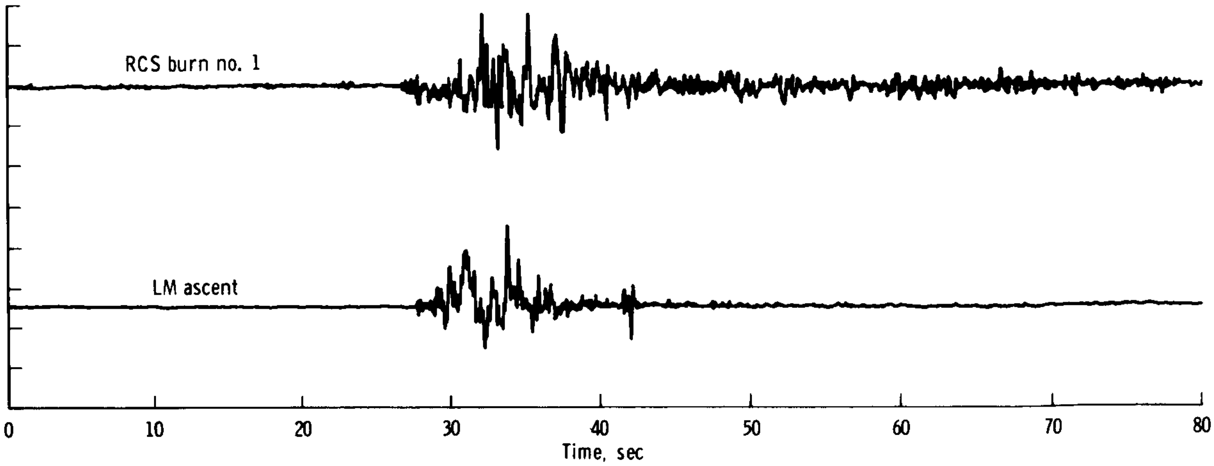

FIGURE 3-5. — Signals recorded during test fire of the RCS thrustors on the lunar surface and during LM ascension.

the main coil of the SPZ component by variations in magnetic flux. These signals will be studied with a view toward the possibility of extending the measurement of magnetic-field variations to higher frequencies than can be recorded with the magnetometer because of its lower data rate.

The two largest events recorded to date are shown on a compressed time scale in figure 3–6 along with the signal from the LM impact, which is to be discussed subsequently. The signals are prolonged (total durations are between 30 min and 1 hr), with the gradual increase and decrease in signal strength that is characteristic of all signals thus far recorded by the LP seismometers. These signals are classified as L-signals according to the nomenclature adopted in the "Apollo 11 Preliminary Science Report" (ref. 3–2). It should be noted that this designation does not refer to a particular type of seismic wave; the designation is simply a shorthand means of referring to the class of signals described. In general, L-signals are complex, with little correlation between the three LP seismometer channels. The familiar pattern of signals corresponding to the various body waves and surface waves typically observed from earthquakes is not observed in any of the recorded signals. However, there is some indication of the arrival of body waves (compressional (P) waves and shear (S) waves) in the early parts of the larger L-signals and in the LM impact signal. It is expected that these phases, although indistinct, can be identified by use of more sophisticated analysis techniques and can be used to determine the velocity structure of the outer regions of the Moon.

Another interesting feature of L-signals is that the peak amplitudes recorded on all three LP seismometers are nearly the same in every case. The spectrum of the largest event (December 10, 1969) is shown in figure 3–7. The spectrum of the signal is broad, with maximum energy near 1.6 Hz. The very-low-frequency peak in the spectrum is produced by an oscillation present on the LPZ seismometer at the time of the event and is not related to the seismic signal.

A very significant event was recorded when the LM ascent stage impacted at a distance of 75.9 km from the ALSEP (azimuth from ALSEP, E 24° S). The angle between the LM trajectory and the mean lunar surface was 3.7° at the point of impact. The azimuth of the trajectory was 305.85°. Signal from the impact was recorded well on all three LP seismometers. The signal amplitude built up gradually to a maximum of 10 nm, peak to peak (all components), over a period of approximately 7 min and thereafter decreased gradually into the background. The total signal duration was approximately 55 min. The signal is shown with a compressed time scale in figures 3–6 and 3–8. Except for the very beginning of the wave train, distinct signals corresponding to various types of seismic waves

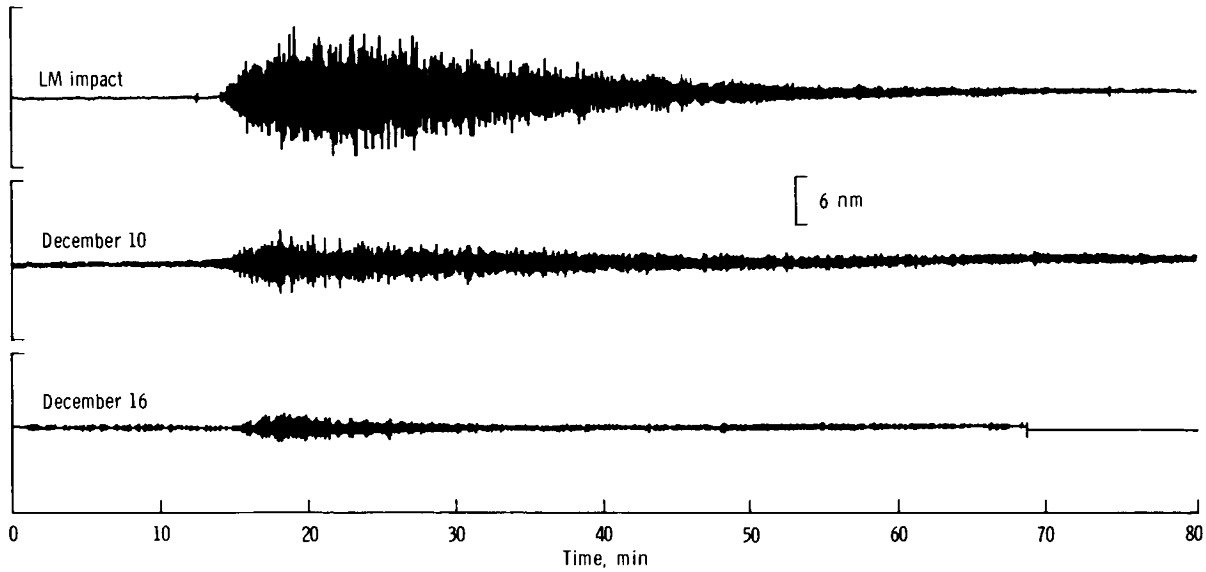

FIGURE 3-6. — The two largest seismic events recorded to date, in compressed time scale, compared with the signal received from the LM impact. Only LPZ components are shown.

(phases) are not apparent. The first few minutes of the filtered and rotated seismograms are shown with an expanded time scale in figure 3–9. The first signal, assumed to be the compressional wave P, is very small in amplitude, and it is difficult to specify the exact arrival time. The prominent signal that occurs near the beginning of the wave train was produced by a sudden tilt of the instrument. Such tilts occurred throughout the recording period, but they are especially prominent at times of terminator crossings. A possible second arrival, marked "S(?)" in figure 3–9, may be the arrival of the direct shear wave.

There is no visible correlation between components after the very first portion of the wave train. A test for coherence was carried out by generating the cross-spectral matrix for the X, Y, and Z components. Figure 3–10 shows power and cross spectra for the first 20 min of the LM impact signal. The data sample starts at 22 hr 17 min 36.43 sec (approximately the onset time of the emergent first arrival) and ends at 22 hr 38 min 12.9 sec. Spectra are normalized to the amplitude of the LPX spectrum, and the raw data were smoothed by the first finite difference (high-pass filtering) before the spectral estimates were computed.

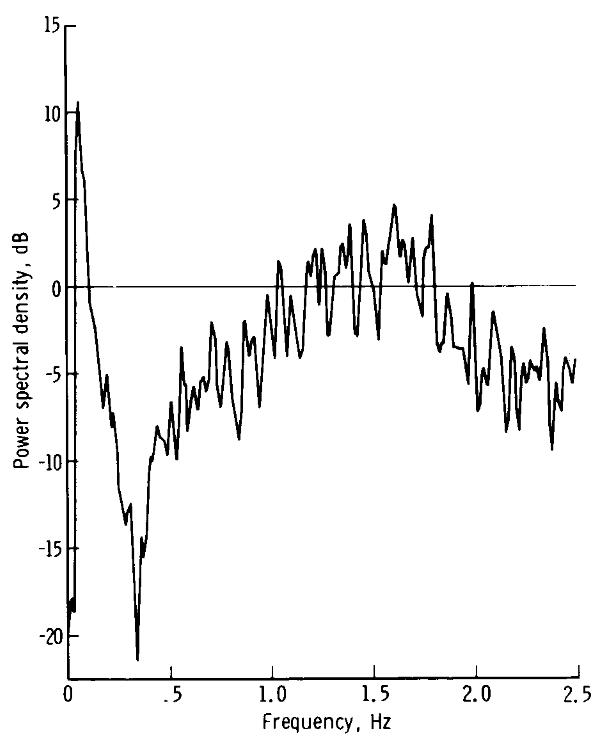

FIGURE 3-7. — Frequency spectrum of the event on December 10, 1969.

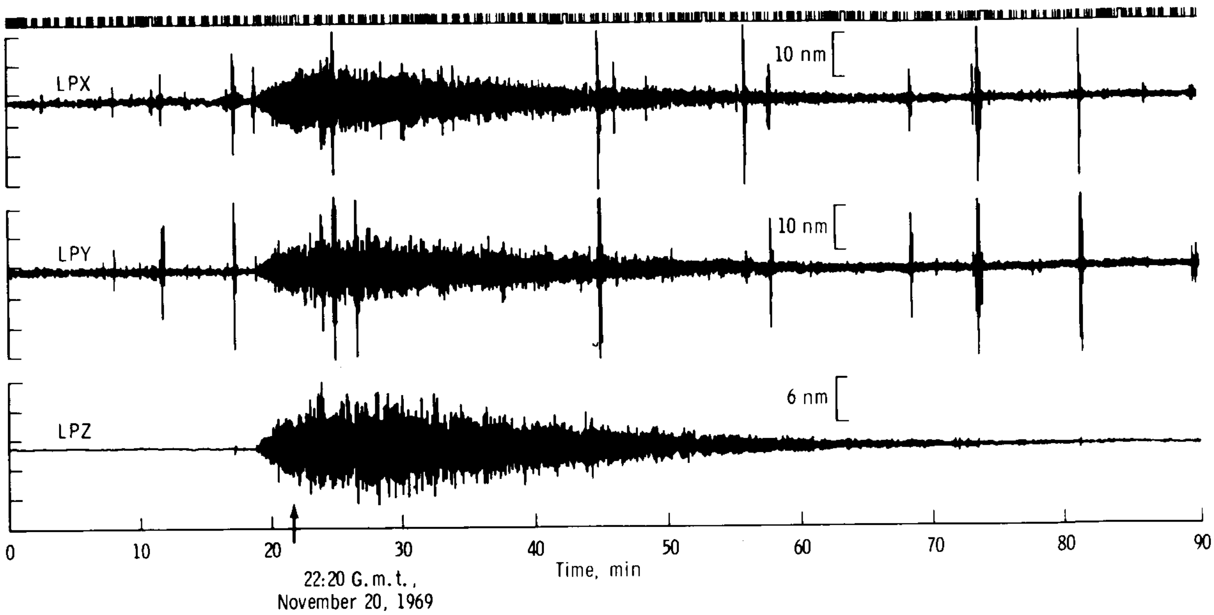

FIGURE 3-8. – Three LP components of the LM impact signal in compressed time scale.

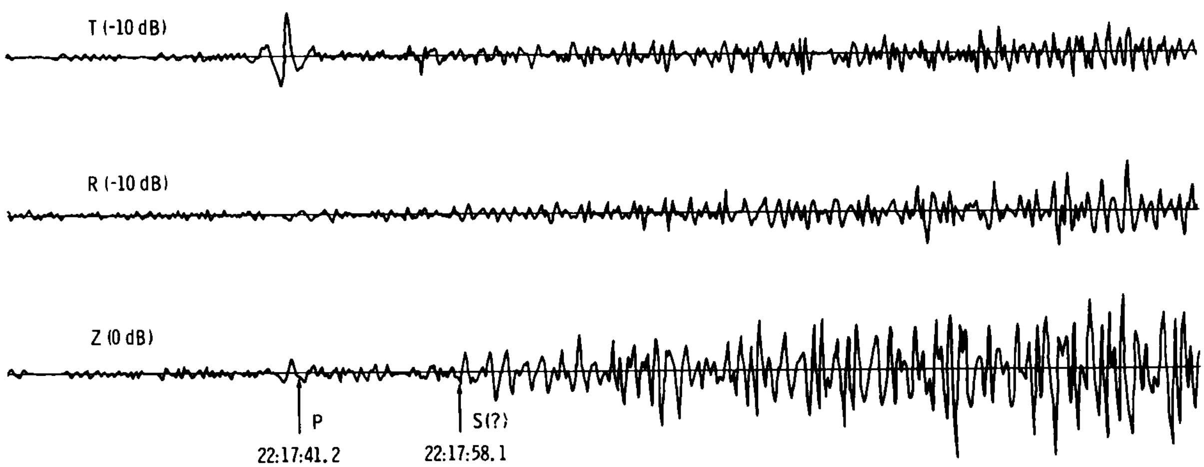

FIGURE 3-9. – Signals from the LM impact in expanded time scale. The data from the two LP horizontal-components seismometers are rotated to give transverse (T) and radial (R) components with respect to the impact point.

In general, the spectra for the LPX, LPY, and LPZ components are broadly centered at 1 Hz, with peaks at 0.95 and 1.2 Hz. The phases of the cospectra between the LPX-LPY and the LPX-LPZ components do not reveal consistent phase relationships between these components. Interestingly, there is some indication of a possible consistent phase relation between the LPY and LPZ components, although shorter time samples of data do not show this correlation. By using the real parts of power spectra and cospectra, the coherence between signal components was computed, using the definition

$$C_{XY} = \left(\frac{S_{XY} \cdot S_{YX}}{S_{XX} \cdot S_{YY}} \right)^{1/2}$$

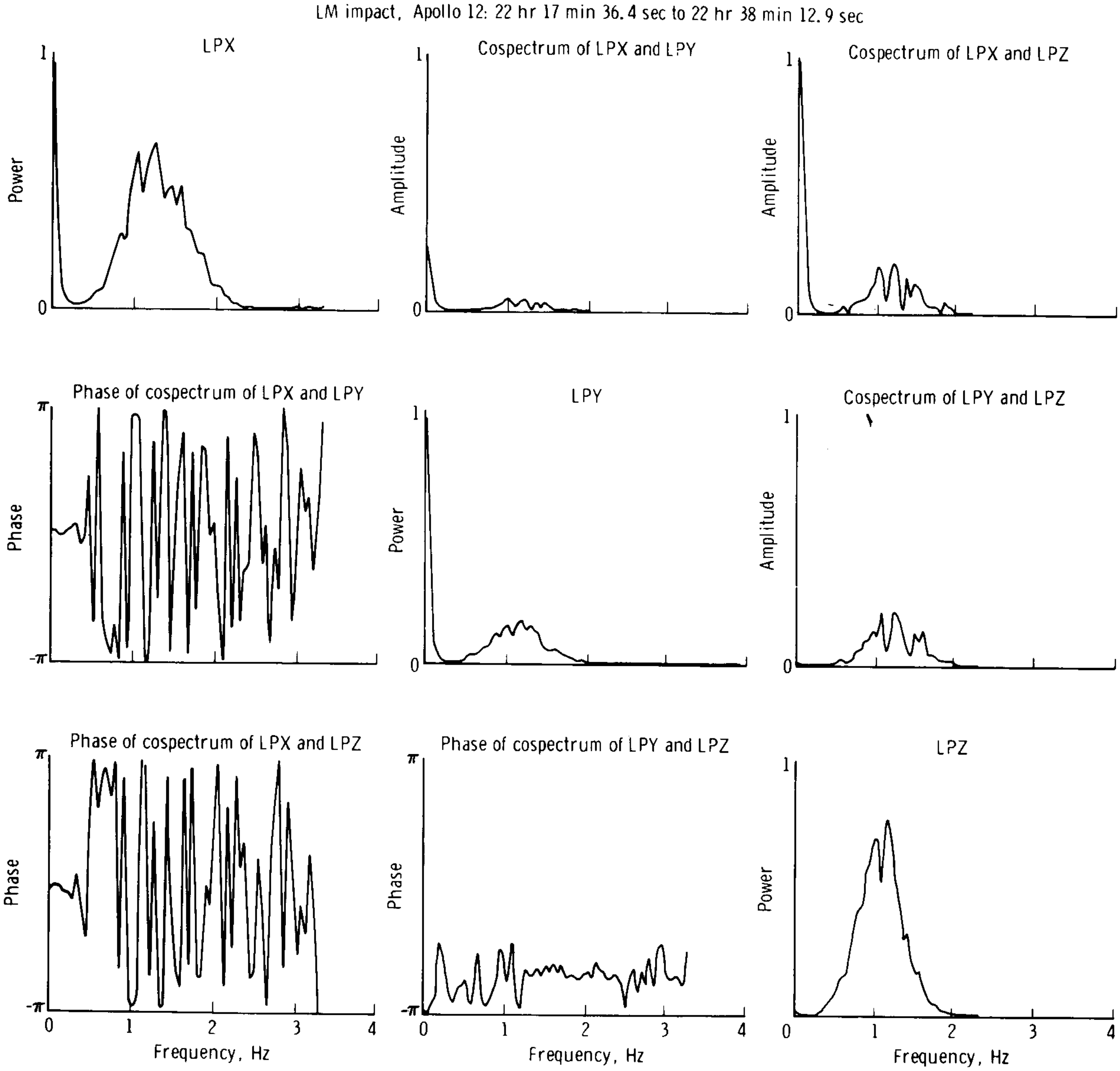

FIGURE 3-10. — Power spectra, cospectra, and phases of cospectra of the three LP components of the LM signal for the first 20 min. The spectral amplitudes are normalized to the LPX spectrum.

where C is coherence, S_{XY} and S_{YX} are cospectra, and S_{XX} and S_{YY} are spectra of X and Y components. In the frequency band of peak power (f=0.5 to 1.5 Hz), the coherence between the LPX-LPY and LPX-LPZ seismometer pairs is quite low ($C<0.5$). The coherence between LPY and LPZ components is somewhat higher ($C \approx 0.6$), indicating a better correlation. These results suggest that during the first 20 min of the impact wave train (1) the coherent motion was primarily P, SV, or Rayleigh type and (2) the primary direction of propagation was from the source (impact site) toward the instrument. The lack of strong coherence between any of the components indicates the presence of interference either between different wave types or between arrivals from different directions owing to reflections or to scattering. No signal was detectable on the SPZ component. This is attributed to the reduced sensitivity of the SPZ seismometer.

The seismic wave velocity corresponding to the first arrival ranges between 3.1 and 3.5 km/sec. The range in velocities is due to the uncertainty in the exact location of the emergent beginning of the wave.

Feedback (Tidal) Outputs and Instrument Temperature

The PSE LP seismometers are sensitive to tilt (horizontal components) and changes in gravity (vertical component). These data are transmitted through separate data channels referred to as "feedback" or "tidal" outputs. Large tilts (0.5 to 1 minute of arc) have been observed during passage of the terminator over the PSE site, when thermal changes are most rapid. When the change is from day to night, tilting begins several hours before local terminator crossing and lasts for several days. When the change is from night to day, tilting begins abruptly at the time of terminator passage and continues for several days. The close correlation between the time of terminator passage and the onset of tilting suggests that such tilts result from thermal effects on the instrument. Rapid heating and cooling of the Mylar thermal shroud is thought to be a major source of these disturbances.

Discussion

The background seismic noise at the Apollo 12 site is frequently not detectable by the PSE; that is, it is below 0.3 nm at 1 Hz. Thus, seismometers can be used on the Moon at much higher sensitivities than could be achieved on Earth. This result was also obtained for the Apollo 11 recording site (refs. 3–2 and 3–3).

The occurrence of similar L-events during both the Apollo 11 and 12 missions greatly strengthens the present belief that, of the various types of signals observed, L-events are most likely to be of natural origin. Equally important, the inclusion of the LM impact signal in this family shows that L-type signals can be generated by impulsive sources on the Moon. This observation suggests that all L-events were produced either by meteoroid impacts or by shallow moonquakes. By comparing the various L-phases with the LM impact signal, it may be concluded that few, if any, L-events originated significantly farther from the seismometer than the LM impact. The LM impact occurred at a distance of 75.9 km. Many, however, appear to have come from smaller distances.

To explain the unexpectedly long duration of the wave train, it must be assumed either that the effective source mechanism was prolonged in some manner or that the long duration of the wave is a propagation effect. An extended source from an impact might result from (1) triggering of rockslides within a crater located near the point of impact, (2) distribution of secondary impacts of ejecta that would presumably rain downrange (toward ALSEP) from the primary impact point, (3) disturbance by an expanding gas cloud consisting of residual LM fuel (180 kg) and volatilized ejecta, and (4) collapse of "fairy castle" or other fragile structures triggered by seismic waves. None of these mechanisms is considered likely, although the possible effects of secondary impacts deserve closer consideration. Since the signal maximum occurred approximately 7 min after impact, it is assumed that the main contribution from secondary impacts would correspond to a time of flight to 7 min for the ejecta. The range from the primary impact point to the secondary impact point can then be computed as a function of the velocity of the ejected particle. The results of this calculation are given in table 3–I. It can be seen from table 3–I that ejecta velocities would have to be less than 0.4 km/sec and the corresponding ejection angle greater than 54° to account for the arrival of

TABLE 3–I. *Distance From Primary Impact Point to Secondary Impact Point as a Function of Ejecta Velocity for a 7-Min Time of Flight*

Ejecta velocity, km/sec	*Ejection angle (from horizontal), deg*	*Range, km*
1.6	1.1	493
1.4	4.4	555
1.2	8.0	460
1.0	12.7	381
.8	19.4	299
.4	54.0	93

secondary impacts in the vicinity of the PSE (range=76 km) 7 min after the impact. These values are well outside the expected range for the shallow impact angle of the LM. (The LM struck the lunar surface traveling at 1.67 km/sec at an angle of 3.7° from the horizontal.) Since the signal produced by the LM impact began approximately 23.5 sec after impact, not all of the signal can be attributed to ejecta landing near the seismometers. The minimum time of flight at near-orbital velocity would be approximately 45 sec. The same remark applies to propellant gases released upon impact. Only seismic wave propagation permits signal velocities high enough to account for the beginning of the disturbance, regardless of the details of the mechanism postulated. In addition, the fact that the same signal character is observed for events of natural origin suggests that the signal character is produced primarily by propagation effects.

If the signal duration is a propagation effect, the attenuation of seismic waves in the lunar material through which these waves traveled must be extremely low. Attenuation of elastic energy in a vibrating system is frequently specified by the quantity Q (quality factor) for the system; or $1/Q$, the dissipation function, where $1/Q$ is the fractional loss of elastic energy per cycle of vibration of the system. Thus, a high Q implies low attenuation. The value of Q for the lunar material in the region of the Apollo 12 site ranges between 3000 and 5000. This range is in contrast with values of Q between 10 and 300 for most crustal materials on Earth.

One hypothesis that could explain the signal character of L-phases is that the Moon not only has a high Q but also is very heterogeneous, at least in its outer regions. Heterogeneity is also implied by surface evidence. The scattering of seismic waves that would occur through a highly heterogeneous material would tend to increase the duration of the observed seismic wave and to suppress the appearance of distinct phases within the wave train. A medium that shows high Q and high scattering efficiency is unlike anything observed within the Earth. Cold blocks of different composition in welded contact might show these properties. A welded aggregate might scatter seismic waves and still maintain high Q. Whatever the mechanism is determined to be, it will provide important evidence on the origin and evolution of the lunar interior.

If the outer region of the Moon is composed of blocks of varying dimensions, seismic waves traveling through this material would be intensely scattered. In the case of extreme scattering, the seismic wave energy may be considered to diffuse through the medium in a manner analogous to the flow of heat through a solid or the movement of gas molecules through a gaseous medium. Such propagation is governed by the laws of diffusion in which, as applied to the present case, the seismic energy "flow" is proportional to the gradient of energy density. The applicable equations are given by Latham et al. (ref. 3–3). This hypothesis can be tested by comparing the observed variation of seismic signal energy from the LM impact with the signal predicted from diffusion theory.

Figure 3–11 is the smoothed envelope of the observed seismic signal from the LM impact plotted on an arbitrary decibel scale. Two theoretical curves based upon diffusion theory are also shown. One curve assumes that the outward

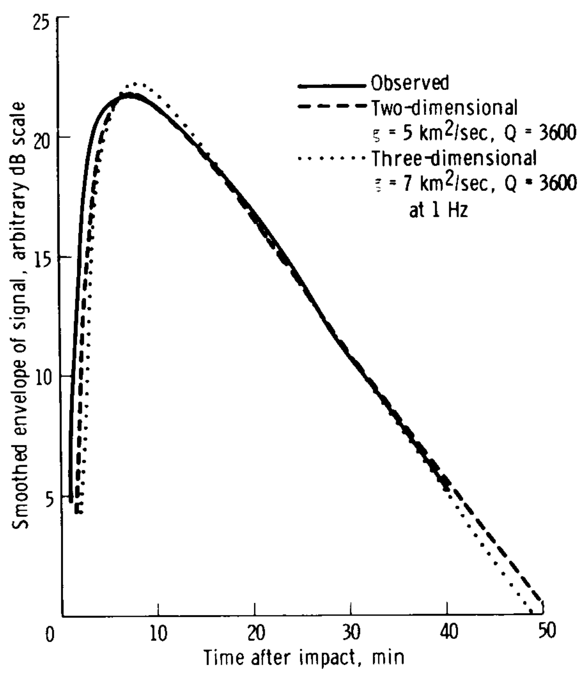

FIGURE 3-11. – Smoothed envelope of the observed wave train from the LM impact compared with the energy distribution with time predicted by diffusion hypothesis.

radiating energy is confined to a near-surface zone (two-dimensional spreading), and the other curve assumes spherical (three-dimensional) spreading. The parameter ξ is the product of a characteristic distance λ, defined as the distance over which one-half of the outward radiating energy is reflected back toward the source, and the average velocity of propagation ν. The symbol Q is the quality factor of the lunar material, as defined previously.

It can be seen from the graph (fig. 3–11) that the diffusion theory accurately predicts the observed signal envelope except for the first few minutes, where the theory predicts somewhat smaller amplitude than is observed. It may be that conventional ray theory provides the best explanation for the early part of the signal. Although this result does not verify the scattering hypothesis, it is sufficiently encouraging to warrant further consideration.

As shown in figure 3–11, the value of ξ that gives the best fit between the theoretical and experimental curves ranges between 5 and 7 km^2/sec. By assuming an average velocity of 3 km/sec and $\xi=6$, the characteristic distance λ is 2 km. This value of λ means that one-half of the propagating seismic energy is reflected back over a distance of 2 km. What this reflection means in terms of the average distribution of discontinuities in the medium is not precisely known. However, it can be assumed that the linear dimension between scattering surfaces must be a fraction of 1 wavelength. The predominant signal frequency is approximately 1 Hz; thus, 1 wavelength is approximately 3 km. Taking 1/10 wavelength to 1 wavelength as limiting values, the inferred separation between discontinuities, or dimensions of blocks, ranges between 300 m and several kilometers. Of course, heterogeneity may exist on a scale outside the range, but would not contribute appreciably to scattering for the observed wavelengths.

The seismic signal detected from the Apollo 12 LM impact (fig. 3–8) demonstrated that prolonged wave trains can be produced on the Moon by relatively small impulsive sources. This result is extremely important to interpretation of the long reverberation as a propagation effect and could be explained by postulating extremely low attenuation (high Q) for the Moon. While the evidence for low attenuation is hard to deny, this phenomenon raises some difficult questions as to its mechanism. Regardless of the explanation of signal duration, the similarity between the impact signal and other prolonged signals suggests that the latter were produced by meteoroid impacts or by near-surface moonquakes at ranges mostly within 100 km of the seismometer.

The seismic energy generated at the point of impact can be calculated from the observed signal amplitude. The calculated energy is on the order of 10^{10} ergs if two-dimensional spreading is assumed and on the order of 10^{11} ergs if three-dimensional spreading is assumed. These values are 10^{-6} and 10^{-5}, respectively, of the kinetic energy of the LM at impact. For these calculations, the signal amplitude at 10 min into the wave train is taken to be 4.2 nm. Simple harmonic motion at a frequency of 1 Hz is assumed. The density of the lunar material is assumed to be 3 g/cm^3, and the effective thickness of the waveguide for the two-dimensional case is taken to be 4 km.

Although the nature of the signals from the LM impact and other L-type events indicates that a considerable amount of scattering of seismic energy has occurred, it is possible that much of the character of the signal can be explained as resulting from propagation through a near-surface waveguide. As mentioned previously, the compressional wave velocity in the regolith near the lunar surface is approximately 100 m/sec. Based upon laboratory measurements on returned lunar rock samples, as discussed in the following paragraphs, this velocity should increase to approximately 6 km/sec at depths of 15 to 20 km, thus forming the lower boundary of the waveguide. Preliminary calculations using ray optics, on simple models consistent with this velocity-depth structure, indicate that the first several minutes of the seismogram can be explained in this manner. Work is continuing on this approach, and at this writing it appears that a reasonable velocity model can be found that will match the major aspects of the records throughout the wave train. Most of the seismic energy from a near-surface source would be trapped in this waveguide. Detailed comparisons between the LM impact signal and other L-signals should allow determination of which of these two possibilities

— scattering or the characteristic of the velocity-depth function — is the more important mechanism in producing the observed wave trains.

To estimate the near-surface properties of the Moon from the available data, lunar seismic velocity models have been constructed on the basis of the measurements of the physical properties of returned lunar samples. (See ref. 3–6.)

Model I assumes the same variation in elastic parameters with pressure (or depth) as measured in the laboratory on a breccia sample. Model III uses the measured properties of a homogeneous igneous rock. Model II is an attempt to combine the properties of the igneous rock and breccia samples to produce a model that will have the elastic parameters of a highly fractured igneous material. For model II, the bulk density is assumed to be that of the igneous sample (approximately 3.1 g/cm^3), and the compressibility is assumed to be that of the breccia sample. Poisson's ratio is assumed to be 0.30 for model II*a* and 0.27 for model II*b*.

The travel time curves for these models are shown in figure 3–12. The corresponding maximum depths of seismic ray penetration are given in table 3–II.

The observed travel times for the first arrival from the LM impact and a later arrival are also plotted, with a range of times indicating the possible reading error. The first arrival is assumed to be the direct P-wave. The wave type of the second arrival, labeled "S(?)," is uncertain. The travel times for these phases fall in between those predicted for the homogeneous igneous model (III) and the fractured igneous model (II). Thus, if it is assumed that the observed phases correspond to direct P- and S-wave propagation, the correct model for the upper 20 km of lunar material in the vicinity of the Apollo 12 landing site must have been a velocity-depth function that falls between those assumed for models II and III but is closer to the homogeneous igneous rock case of model III. This result must be taken to be very tentative since sample-to-sample variations may be large enough that a single predominant rock type may also be found to fit the observations.

The average rates of L-events detected during the Apollo 11 and 12 recording periods are 4 per day and 0.8 per day, respectively. These rates are

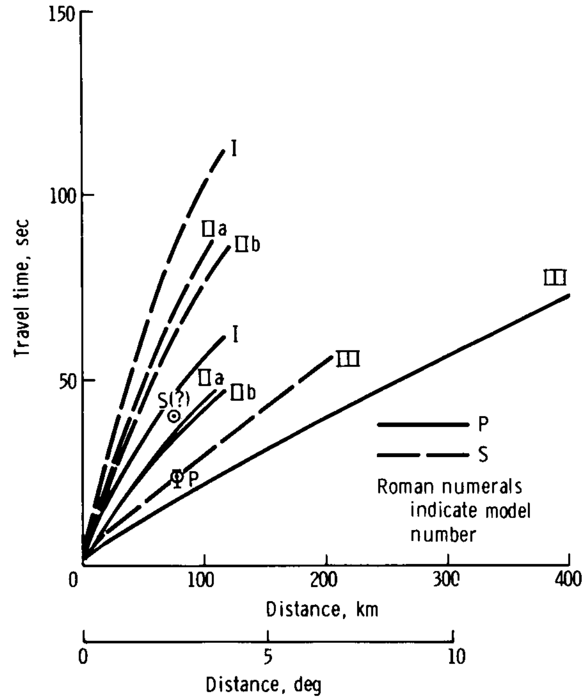

FIGURE 3-12. — First and second arrivals from the LM impact plotted on the travel-time-distance curves based on Apollo 11 lunar sample data from reference 3-6.

consistent with the numbers of detectable meteoroid impacts predicted (refs. 3–7 and 3–8) for a high-*Q* Moon. Thus, it is possible that all of the observed L-signals were produced by meteoroid impacts. The difference in the observed rates of these events on the two missions may result from failure of the Apollo 12 SPZ seismometer to respond to small signals, as discussed previously. Most of the Apollo 11 L-signals were detected by the SPZ seismometer because the predominant frequencies of these signals are higher than the high-frequency limit (2 Hz) of the LP seismometers.

TABLE 3–II. *Depth of Ray Penetration of Rays That Emerge at a 75.9-km Range*

Model	*P-wave depth, km*	*S-wave depth, km*
I	18	21
II*a*	15	15
II*b*	17	17
III	11	8

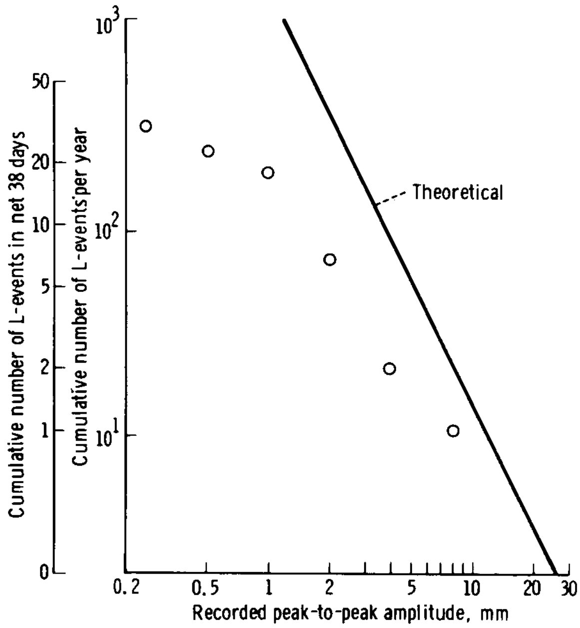

FIGURE 3-13. — Cumulative number of L-events observed to date (denoted by circles). Theoretical curve based on the estimate of meteoroid flux from reference 3-9 is shown by a solid line.

In figure 3–13, the cumulative number of Apollo 12 L-events detected to date by the LP seismometers is compared with the predicted number of detectable meteoroid impacts. The predicted number of impacts assumes (1) the meteoroid flux estimates given by Hawkins (ref. 3–9), (2) attenuation of seismic signals with distance as given by the diffusion model described previously, and (3) that the fraction of impact kinetic energy that is converted to seismic wave energy is the same as that calculated for the LM impact. The conversion efficiency for meteoroids with trajectories more nearly perpendicular to the surface than that of the LM may well be greater than the LM impact efficiency.

In view of the order-of-magnitude estimates involved in these calculations and the short recording time available, the agreement between predicted meteoroid impact signals and the observed data is remarkable. The lack of agreement for small-amplitude signals is probably explained by the inability of the SPZ seismometer to detect small signals. It is concluded from this comparison that there are sufficient numbers of meteoroid impacts to explain all of the observed L-signals as being of meteoroid impact origin, although the presence of some events with other source mechanisms (i.e., moonquakes) is certainly not precluded. By extrapolating the results given in figure 3–13 to large amplitudes, signals with amplitudes equal to that of the LM impact signal are expected to occur at an average rate of three per year.

Few, if any, of the observed signals have patterns normally observed in recordings of seismic activity on Earth (with the possible exceptions of volcanic tremors, microseisms, and landslide signals; i.e., signals from sources that have extended source mechanisms). Phases corresponding to the various familiar types of body and surface waves are either indistinct or absent in the lunar signals, and most wave trains are of long duration with little phase correlation between components.

The fact that no seismic signals with characteristics similar to those typically recorded on the Earth were observed during the combined recording period for Apollo 11 and 12 (63 days at this writing) is a major scientific result. The high sensitivity at which the lunar instruments were operated would have resulted in the detection of many such signals if the Moon were as seismically active as the Earth and had the same transmission characteristics as the Earth. Thus, the data obtained indicate that either seismic energy release is far less for the Moon than for the Earth or the deep interior of the Moon is highly attenuating for seismic waves. Although the material of the outer region of the Moon (to depths of at least 20 km) appears to exhibit very low attenuation in the regions studied, the possibility of the existence of high attenuation at greater depths cannot presently be excluded. The absence of significant seismic activity within the Moon, if verified by future data, would imply the absence of tectonic processes similar to those associated with major crustal movements on the Earth and would imply lower specific thermal energy in the lunar interior than is present in the interior of the Earth.

Interpretation of present data is not concerned with the structure of the deep interior of the Moon since most of the recorded events appear to have occurred at relatively short ranges. The relatively thick zone of self-compaction in which elastic wave velocity increases strongly with depth would perhaps be 20 km thick. The large increase in velocity with depth results in a surface sound channel that may carry the seismic energy of these events. The impact of the Saturn IVB (SIVB) stage in April 1970, at a range of 200 km from the Apollo 12 ALSEP, should enable extension of present interpretation to depths approaching 50 km into the Moon.

It is also important to remember that all results obtained thus far pertain to mare regions. Quite different results may be obtained for nonmare regions in which the structure may differ radically from that of the mare.

With data from one or two lunar seismic stations, construction of a picture of the lunar interior with detail approaching that of Earth models cannot be expected. Seismic experiments have, nevertheless, already revealed some unexpected phenomena, the understanding of which will eventually answer some important questions concerning the structure and dynamics of the Moon with significant implications for lunar history. As a result of the reduced level of detectable lunar seismic activity relative to Earth, results will come more slowly than had been hoped, and there will be greater dependence upon the establishment of a network of stations and upon use of artificial sources such as impacts of the SIVB stage and the LM ascent stage.

Meteoroid impacts are a major factor in shaping the lunar surface. Determination of the size and frequency distribution of meteoroid impacts is necessary to estimate quantitatively the rates of crater formation and erosion. The lunar seismic experiments will provide data that will be uniquely suited to the study of this problem.

References

3-1. LATHAM, G.; EWING, M.; PRESS, F.; and SUTTON, G.: The Apollo Passive Seismic Experiment. Science, vol. 165, no. 3890, July 18, 1969, pp. 241-250.

3-2. LATHAM, G. V.; EWING, MAURICE; et al.: Passive Seismic Experiment. Sec. 6 of Apollo 11 Preliminary Science Report, NASA SP-214, 1969, pp. 143-161.

3-3. LATHAM, G. V.; et al.: Apollo 11 Passive Seismic Experiment. Science, vol. 167, no. 3918, Jan. 30, 1970, pp. 455-457.

3-4. CHRISTENSEN, E. M.; BATTERSON, S. A.; et al.: Lunar Surface Mechanical Properties at the landing Site of Surveyor 3. J. Geophys. Res., vol. 73, no. 12, June 15, 1968, pp. 4081-4094.

3-5. CHOATE, R.; BATTERSON, S. A.; et al.: Lunar Surface Mechanical Properties. Sec. 4 of Surveyor Program Results, NASA SP-184, 1969, pp. 129-169.

3-6. SCHREIBER, E.; et al.: Sound Velocity and Compressibility for Lunar Rocks 17 and 46 and for Glass Spheres From the Lunar Soil. Science, vol. 167, no. 3918, Jan. 30, 1970, pp. 732-734.

3-7. LASTER, S. J.; and PRESS, F.: A New Estimate of Lunar Seismicity Due to Meteorite Impact. Phys. Earth and Planet Interiors, vol. 1, 1968, pp. 151-154.

3-8. MCGARR, A.; LATHAM, G. V.; and GAULT, D. E.: Meteoroid Impacts as Sources of Seismicity on the Moon. J. Geophys. Res., vol. 74, no. 25, Nov. 15, 1969, pp. 5981-5994.

3-9. HAWKINS, GERALD S.: The Meteor Population, Research Report No. 3. NASA CR-51365, Aug. 1963.